

Economic MPC with an Online Reference Trajectory for Battery Scheduling Considering Demand Charge Management

Cristian Cortes-Aguirre*, Graduate Student Member, IEEE, Yi-An Chen*, Avik Ghosh, Graduate Student Member, IEEE, Jan Kleissl, and Adil Khurram, Member, IEEE

Abstract—Monthly demand charges form a significant portion of the electric bill for microgrids with variable renewable energy generation. A battery energy storage system (BESS) is commonly used to manage these demand charges. Economic model predictive control (EMPC) with a reference trajectory can be used to dispatch the BESS to optimize the microgrid operating cost. Since demand charges are incurred monthly, EMPC requires a full-month reference trajectory for asymptotic stability guarantees that result in optimal operating costs. However, a full-month reference trajectory is unrealistic from a renewable generation forecast perspective. Therefore, to construct a practical EMPC with a reference trajectory, an EMPC formulation considering both non-coincident demand and on-peak demand charges is designed in this work for 24 to 48 h prediction horizons. The corresponding reference trajectory is computed at each EMPC step by solving an optimal control problem over 24 to 48 h reference (trajectory) horizon. Furthermore, BESS state of charge regulation constraints are incorporated to guarantee the BESS energy level in the long term. Multiple reference and prediction horizon lengths are compared for both shrinking and rolling horizons with real-world data. The proposed EMPC with 48 hour rolling reference and prediction horizons outperforms the traditional EMPC benchmark with a 2% reduction in the annual cost, proving its economic benefits.

Index Terms—Economic model predictive control, reference trajectory, demand charge, microgrid, energy storage, battery

NOMENCLATURE

\mathbf{u}_1	Vector of $u_1(t)$ for all $t \in \mathbb{T}$
\mathbf{u}_{r1}	Vector of $u_{r1}(t)$ for all $t \in \mathbb{T}$
$\hat{y}_{\text{NC}}, \hat{y}_{\text{OP}}$	Future NC/OP reference trajectory peak
ΔT	Time step
η	Roundtrip efficiency
$\hat{\tau}_{\text{MPC},t}, \hat{\tau}_{\text{R},t}$	Time point where the 50% SOC low threshold is placed in a prediction/reference horizon
\hat{k}	Time point where the reference trajectory was computed
$\hat{P}_{\text{NC}}, \hat{P}_{\text{OP}}$	Monthly DCT for NC/OP demand charge
$\hat{y}_{\text{NC}}, \hat{y}_{\text{OP}}$	NC/OP reference trajectory peak
\mathbb{T}	Set of discrete time points
$\mathbb{T}_{\text{NC}}, \mathbb{T}_{\text{OP}}$	Set of the first time points of all $\mathcal{T}_{\text{NC},t}/\mathcal{T}_{\text{OP},t}$
\mathcal{C}_1	Energy cost
\mathcal{C}_2	Demand charge cost
\mathcal{T}_t	Set of all time points in the month that t belongs to
$\mathcal{T}_{\text{MPC},t}, \mathcal{T}_{\text{R},t}$	Set of all time points corresponding to the prediction/reference horizon starting at the time point t

$\mathcal{T}_{\text{NC},t}, \mathcal{T}_{\text{OP},t}$	Set of all time points corresponding to NC/OP demand charge periods for the month \mathcal{T}_t
\bar{u}_2	BESS power capacity
\bar{x}, \underline{x}	BESS SOC limits
$\sigma_{\text{NC}}, \sigma_{\text{OP}}$	Binary variable to identify the beginning of $\mathcal{T}_{\text{NC},t}/\mathcal{T}_{\text{OP},t}$
$\tau_{\text{MPC},t}, \tau_{\text{R},t}$	Final time point of the set $\mathcal{T}_{\text{MPC},t}/\mathcal{T}_{\text{R},t}$
$\tau_{\text{NC},t}, \tau_{\text{OP},t}$	Final time point of the set $\mathcal{T}_{\text{NC},t}/\mathcal{T}_{\text{OP},t}$
$\tau_{e,t}$	Final time point of a specific (future) horizon
BESS_{en}	BESS energy capacity
k, k'	Prediction/Reference horizon time point
L	Stage cost
L_f, PV_f	Forecasted load/PV generation
$P_{\text{NC}}, P_{\text{OP}}$	NC/OP peak demand within the set $\{t, \dots, \tau_{e,t}\}$
R_{EC}	Energy charge rate
$R_{\text{NC}}, R_{\text{OP}}$	NC/OP demand charge rate
t	Time point
$T_{\text{R}}, T_{\text{MPC}}$	Reference/Prediction horizon length
u_1	Demand
u_2	BESS charging/discharging power
u_{r1}	Reference trajectory's demand
u_{r2}	Reference trajectory's BESS charging/discharging power
V_f	Terminal cost function
x	BESS SOC
x_r	Reference trajectory BESS SOC
$y_{\text{NC}}, y_{\text{OP}}$	NC/OP peak demand tracker
z	Augmented state of the proposed EMPC formulation
z_r	State and control inputs used as a reference trajectory
BESS	Battery energy storage system
DCM	Demand charge management
DCT	Demand charge threshold
EMPC	Economic MPC
EV	Electric vehicle
MG	Microgrid
MPC	Model predictive control
NC	Non coincident
NCDC	NC demand charge cost
NT, WT	Without/With peak demand tracking
OP	On peak
OPDC	OP demand charge cost
PV	Photovoltaic
SAM	System advisor model
SOC	State of charge
VRE	Variable renewable energy

*: These authors contributed to the paper equally

I. INTRODUCTION

In the US and other parts of the world, the electricity tariff for most commercial consumers includes a monthly demand charge, which is calculated based on the highest average load requested from the grid, measured in kW, within a 15-minute interval of the monthly billing period [1]. Demand charge rates are usually one to two orders of magnitude higher than energy charge rates [2]–[4]. Thus, demand charge management (DCM) based on economic cost minimization is attractive in sizing, day-ahead planning and real-time operation of microgrids.

The effective management of BESS or flexible loads can mitigate demand spikes for customers operating microgrids with high penetration of variable renewable energy (VRE) resources. Works such as [5] describe the mathematical formulation and demonstrates the potential of REopt LiteTM [6], [7], a web-based mixed integer programming optimization tool to optimally size and dispatch VRE, conventional generation and storage installations in a microgrid. However, as clarified by the authors in [5], models like REopt Lite work in a deterministic framework, optimizing over a representative year, where the weather (VRE resource data) and load for the entire year is known perfectly (or taken from a baseline) a-priori. While the deterministic framework makes REopt a powerful and computationally efficient tool for microgrid design, it is not adept for usage in real-time microgrid control where prediction horizons are much shorter than a year (typically 24 – 48 h) with the possibility of forecasts being imperfect which needs to be accommodated by the system in real-time.

While demand charges are calculated on a monthly basis, for real-time microgrid control, shifting the power requested from the grid (called demand) from higher demand hours to lower demand hours on a daily basis through a battery energy storage system (BESS) can lower monthly peak demand [8]. With the adoption of VRE sources, such as wind, solar, and electric vehicle (EV) charging stations, net loads have generally become more variable, and DCM with BESS has received much interest in the literature. BESS assisted DCM is applied in commercial and industrial buildings in [9], [10], residential buildings in [11]–[13], utility-scale sites in [14], [15], and at EV charging sites [16]–[19] and are often combined with PV generation [9]–[11].

One of the most common BESS control strategies for DCM is model predictive control (MPC), broadly subdivided into tracking and economic MPC. Tracking MPC computes control actions that minimize the deviation of the system operating point from a desired trajectory (or point) subject to input and state constraints over a finite prediction horizon. The inputs to the MPC are the latest state realizations (or observations) and forecasts of time-varying constraint parameters. At every time step, after computing the control actions for the entire prediction horizon, only the first control action is implemented. Then the system evolves to the next time step accordingly, and the optimization is repeated with updated inputs. However, the cost function and the desired trajectory in tracking MPC do not necessarily correspond to economic cost. Tracking MPC instead relies on the pre-computed trajectory to minimize

demand charges. Defining a desired trajectory a-priori, for the system to follow in real-time for DCM, is challenging.

Another way to optimize BESS dispatch for DCM is to directly use the economic cost function as the objective function over the prediction horizon, which is known as economic MPC (EMPC) [20]. This approach was used by the authors in [21], [22] where the objective function is the electricity cost, composed of energy charges and demand charges. Note that, in reality, the demand charge is levied at the end of the month based on the maximum demand over the entire month, while the prediction horizon is shorter than a month (typically between 24 and 48 h). This mismatch of timescales can lead to greedy control actions toward the peak demands within the current prediction horizon, even when a much larger peak had already occurred during previous days of the month. These greedy control actions can result in BESS not having enough energy for the next high demand period, which can increase the peak demand, and the greedy control actions can also increase the BESS losses and degradation cost due to unnecessary BESS dispatch. Therefore, EMPC needs to keep track of the past peaks within the month to avoid greedy control actions. Previous works such as [21], [22] do not consider past peaks and implement the EMPC solutions naively in real-time, while other studies do not consider demand charges, which is unrealistic for many commercial consumers [23], [24].

Different approaches have been used in the literature to track previous peak demands. Some studies include a demand charge threshold (DCT) in the daily optimization algorithm [8]–[18] and the DCT is adjusted in real time in [8], [10], [13], [15]–[18]. An initial value of DCT can be set at the beginning of the month, either based on historical data or expert knowledge. During the simulation throughout the month, DCT is included in the demand charge term of the cost function. After each time step, DCT is updated with the highest demand up to the current time step, storing the memory of the highest peak of the month. Then, only when the forecasted demand is higher than the DCT, the BESS is scheduled to dispatch to prevent higher peak demands. [8] first optimizes the persistence forecasted load to determine a daily DCT, which is then updated within the day in real time based on measurements. [10], [13] estimate a monthly DCT from past measurements. While [10] adds a penalty for DCT violations to the cost function of an MPC, [13] updates the DCT during the day based on BESS constraints and demand forecast. [16] sets the initial monthly DCT to be zero and updates DCT in real time. [17] defines the demand charge cost term as the difference between the DCT computed up to the current time step and the predicted peak within the prediction horizon. [15] incorporates a discount factor to split the total demand charge cost (based on a DCT) equally among the prediction horizon time points. Finally, [18] also applies the discount factor of [15] in the demand charge cost term, but also considers an estimation of future peaks beyond the prediction horizon based on historical measurements. While the above traditional EMPCs with peak tracking reduce demand charge costs and battery cycling compared to traditional EMPCs without peak demand tracking, including a reference trajectory as an input to the EMPC formulation, can also lower electricity

costs. A reference trajectory in EMPC has desirable closed-loop properties, such as asymptotic stability and performance guarantees [25].

The reference trajectory is a set of feasible states and control actions over the entire horizon. It can be derived from higher layers of long-term optimization for grid operators to design the objective functions for short-term optimizations. The long-term targets include economic, and safety objectives, and the short-term optimization considers the grid's operational constraints while following the dispatch plan [26], [27]. When the short-term cost function is known and the forecast for the PV generation and load is available, the reference trajectory consists of states and control actions from the first optimization layer for the MPC to track and improve the system's economic performance [28]. [25] first applied EMPC with a pre-defined monthly reference trajectory for DCM. A terminal cost and constraint are defined in the EMPC based on the reference trajectory. The EMPC also incorporated demand charge costs by including an auxiliary state. The auxiliary state tracks not only the previously achieved peaks but also tracks peaks within the prediction horizon. Under continuity and strict dissipativity assumptions [25], the reference trajectory can guarantee stability and provide an upper bound to the average cost. These assumptions can be satisfied by the BESS.

The reference trajectory benefits the EMPC in two aspects. (1) Knowledge about the system state and control actions from outside the prediction horizon is incorporated into the MPC. (2) The reference trajectory provides a first approach to the optimal control action that allows modifications on SOC regulation constraints when tracked by the EMPC afterward. A drawback of [25] is the requirement of a full-month reference trajectory a-priori. A full-month reference trajectory is not practical because it requires knowledge about the MPC inputs (e.g., load, renewable energy generation) weeks in advance which is hard to obtain. In particular, renewable energy generation forecasts up to 24 or 48 h in advance are more practical.

Inspired by [25], we propose an optimal BESS scheduling model for DCM based on an EMPC algorithm as shown on the right side of Fig. 1. In the proposed EMPC algorithm, the reference trajectory is updated online and then used in the terminal cost and constraint. The work involves two stages: (i) In the reference stage, we obtain a reference trajectory consisting of BESS state of charge (SOC) and control actions by solving an optimization problem, which includes a 50% SOC low threshold as a SOC regulation constraint, with and without peak demand tracking over a practical reference trajectory horizon (24 and 48 h); and (ii) In the MPC stage, we run an EMPC with a terminal cost and a terminal SOC constraint over a prediction horizon using the reference trajectory from (i) as input to the EMPC. Finally, we implement only the first control action obtained from (ii), allow the system to evolve, and repeat the process from (i). The performance of the proposed EMPC algorithm is compared with a traditional EMPC without a reference trajectory (EMPC framework presented on the left side of Fig. 1). Both algorithms are compared under different configurations: (i) with and without incorporating the memory of the monthly peak demand, (ii) for 24 and 48 h horizon

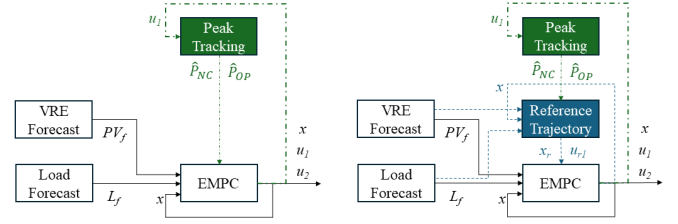


Fig. 1. EMPC frameworks that include load and VRE forecasts, peak tracking, and reference trajectory methods for traditional (left) and proposed (right) EMPC. The following variables are presented: SOC of the BESS (x), charging/discharging power of the BESS (u_2), demand imported from the grid (u_1), forecasted load (L_f), forecasted PV generation (PV_f), NC and OP peak demands (\hat{P}_{NC} and \hat{P}_{OP}), SOC of the BESS estimated as the reference trajectory (x_r), and demand imported from the grid estimated as the reference trajectory ($u_{r,1}$).

lengths, and (iii) with shrinking and rolling horizons.

The contributions of this work are as follows:

- 1) Contrary to [25] where the reference trajectory is assumed a-priori for the entire month, we propose a practical reference trajectory horizon equal to 24 or 48 h, in line with real-world applications. The reference trajectory is updated at each time step by solving an optimal control problem where peak demand tracking compensates for the timescale mismatch between the reference trajectory horizon and the demand charge billing cycle.
- 2) We compare the performance of traditional versus proposed EMPC with and without peak demand tracking for shrinking and rolling horizons using real data. Both 24 and 48 h horizon lengths are considered. Simulation results demonstrate that extending the reference trajectory horizon improves the proposed EMPC performance. Furthermore, the proposed EMPC shows superior performance than the traditional EMPC implemented over a 48 h reference and prediction horizons, with and without peak demand tracking and for shrinking and rolling horizons.
- 3) The proposed EMPC extends the work in [25] to incorporate into the EMPC both non-coincident peak demand and on-peak demand charges, which resembles common electricity tariffs. [25] only considered non-coincident demand charges.

The rest of the paper is organized as follows. Section II presents the traditional and proposed EMPC algorithms, as well as the optimal control problem solved to generate the reference trajectory in the proposed EMPC. Section III presents the simulated case study. Simulation results are discussed in Section IV. Finally, Section V concludes the paper.

II. METHODOLOGY

A. Time scheme

Let \mathbb{T} be the set of time points as shown in Fig. 2, where $t \in \mathbb{T}$ is a time point. Since the demand charge horizon is equal to the entire month, for a given t , \mathcal{T}_t is defined as the set of all time points in the month that t belongs to. This work considers two demand charge peaks: (i) the monthly non-coincident (NC) peak demand, which is the highest average

power demand in any 15-minute interval of the month, and (ii) the on-peak (OP) peak demand, which is the highest average power demand of a 15-minute interval during 16:00 h to 21:00 h of the month. $\mathcal{T}_{\text{NC},t}$ and $\mathcal{T}_{\text{OP},t}$ are defined as subsets of \mathcal{T}_t containing all time points corresponding to NC and OP demand charge periods for the entire month. Note that $\mathcal{T}_{\text{OP},t}$ is a disconnected set, as shown in Fig. 2. The time points corresponding to the prediction horizon at the current MPC step t are collected in $\mathcal{T}_{\text{MPC},t}$ and T_{MPC} is the prediction horizon length. Similarly, the time points corresponding to the reference trajectory horizon (called reference horizon) are collected in $\mathcal{T}_{\text{R},t}$ and T_{R} is the reference horizon length. The time points $\tau_{\text{NC},t}$ and $\tau_{\text{OP},t}$ correspond to the final time points of $\mathcal{T}_{\text{NC},t}$ and $\mathcal{T}_{\text{OP},t}$, respectively, and are used to reset the demand charges at the end of the month. Lastly, $\tau_{\text{MPC},t}$ and $\tau_{\text{R},t}$ are the final time points of $\mathcal{T}_{\text{MPC},t}$ and $\mathcal{T}_{\text{R},t}$, respectively.

Note that the reference horizon $\mathcal{T}_{\text{R},t}$ and the prediction horizon $\mathcal{T}_{\text{MPC},t}$ represent different sets of time points. While both horizons may start at the same time point t , $\mathcal{T}_{\text{R},t}$ corresponds to the time period over which the reference trajectory is computed (further explanation provided in Section II-F). Conversely, $\mathcal{T}_{\text{MPC},t}$ defines the prediction horizon over which an MPC algorithm is defined. As expected, $\mathcal{T}_{\text{R},t}$ and $\mathcal{T}_{\text{MPC},t}$ will correspond to the same time period for cases where both have the same length. Note that we refer to the MPC horizon as the prediction horizon.

B. Electricity cost

A microgrid (MG) containing a BESS and a PV plant schedules the BESS to minimize the cost of electricity purchased from the grid. The electricity cost is assessed monthly and includes the energy cost and two peak demand charge costs. At each $t \in \mathbb{T}$, the energy cost is formulated as

$$\mathcal{C}_1(u_1(t), u_2(t)) = R_{\text{EC}} \Delta T \left(u_1(t) + \frac{(1-\eta)}{2} |u_2(t)| \right), \quad (1)$$

where R_{EC} is the energy charge rate, ΔT is the time step size, and η is the roundtrip efficiency of the BESS. The first term in (1) is the cost of the energy purchased from the grid excluding BESS losses, with u_1 as the demand or power imported from the grid. The second term represents the BESS losses, with u_2 as the charging/discharging power of the BESS ($u_2 > 0$ when the BESS is discharging and $u_2 < 0$ when the BESS is charging). The energy loss at each charging and discharging step is estimated as $R_{\text{EC}} \Delta T (1-\eta) |u_2(t)|/2$. The factor of 1/2 is included to correct for double-counting of energy losses over one charging and discharging cycle, as the implemented formulation does not differentiate between charging and discharging steps. It is assumed that the utility allows the MG to sell back electricity at the energy charge rate.

The demand charge cost term is given by,

$$\begin{aligned} \mathcal{C}_2(\mathbf{u}_1, \hat{P}_{\text{NC}}(t), \hat{P}_{\text{OP}}(t), t, \tau_{e,t}) = & \quad (2) \\ & R_{\text{NC}} \max\{P_{\text{NC}}(\mathbf{u}_1, t, \tau_{e,t}), \hat{P}_{\text{NC}}(t)\} + \\ & R_{\text{OP}} \max\{P_{\text{OP}}(\mathbf{u}_1, t, \tau_{e,t}), \hat{P}_{\text{OP}}(t)\}, \end{aligned}$$

where R_{NC} and R_{OP} are the NC and OP demand charge rates, respectively. \mathbf{u}_1 is a vector where each element corresponds to $u_1(t)$ for all $t \in \mathbb{T}$, and $\tau_{e,t} \in \mathbb{T}$ is the final time point of a specific (future) horizon starting at t where \mathcal{C}_2 is evaluated. In (2), \hat{P}_{NC} and \hat{P}_{OP} are the DCTs that track the NC and OP peak demands (u_1 peaks) observed up to time t , respectively. Similarly, P_{NC} and P_{OP} are the NC and OP peak demands in the horizon defined by t and $\tau_{e,t}$. These peaks are defined as,

$$\hat{P}_{\text{NC}}(t+1) = (1 - \sigma_{\text{NC}}(t+1)) \max\{\hat{P}_{\text{NC}}(t), u_1(t)\} \quad (3a)$$

$$\hat{P}_{\text{OP}}(t+1) = \begin{cases} (1 - \sigma_{\text{OP}}(t+1)) \max\{\hat{P}_{\text{OP}}(t), u_1(t)\} \\ \quad \text{if } t \in \mathcal{T}_{\text{OP},t} \\ (1 - \sigma_{\text{OP}}(t+1)) \max\{\hat{P}_{\text{OP}}(t), 0\} \\ \quad \text{otherwise,} \end{cases} \quad (3b)$$

$$P_{\text{NC}}(\mathbf{u}_1, t, \tau_{e,t}) = \max_{k \in \{t, \dots, \tau_{e,t}\} \cap \mathcal{T}_{\text{NC},t}} u_1(k) \quad (4a)$$

$$P_{\text{OP}}(\mathbf{u}_1, t, \tau_{e,t}) = \begin{cases} \max_{k \in \{t, \dots, \tau_{e,t}\} \cap \mathcal{T}_{\text{OP},t} u_1(k) \\ \quad \text{if } \{t, \dots, \tau_{e,t}\} \cap \mathcal{T}_{\text{OP},t} \neq \emptyset \\ 0 \quad \text{otherwise,} \end{cases} \quad (4b)$$

where $\{t, \dots, \tau_{e,t}\} \cap \mathcal{T}_{\text{NC},t}$ ($\{t, \dots, \tau_{e,t}\} \cap \mathcal{T}_{\text{OP},t}$) is the set of time points between t and $\tau_{e,t}$ that also belong to the NC (OP) demand charge periods. The demand charges consist of NC and OP charges, however, (2) can easily be modified to fit a different cost structure, e.g. [15], [17]. Assuming that neither expert knowledge nor historical demand data are available to determine an initial threshold at the beginning of the month for peak demands, $\hat{P}_{\text{NC}}(0)$ and $\hat{P}_{\text{OP}}(0)$ are set to zero. σ_{NC} and σ_{OP} are binary variables used to reset $\hat{P}_{\text{NC}}(t)$ and $\hat{P}_{\text{OP}}(t)$ at the beginning of each month

$$\sigma_{\text{NC}}(t) = \begin{cases} 1 & \text{if } t \in \mathbb{T}_{\text{NC}} \\ 0 & \text{otherwise,} \end{cases} \quad (5a)$$

$$\sigma_{\text{OP}}(t) = \begin{cases} 1 & \text{if } t \in \mathbb{T}_{\text{OP}} \\ 0 & \text{otherwise,} \end{cases} \quad (5b)$$

where $\mathbb{T}_{\text{NC}} = \{0\} \cup \{\tau_{\text{NC},t} + 1 | t \in \mathbb{T}\}$ ($\mathbb{T}_{\text{OP}} = \{0\} \cup \{\tau_{\text{OP},t} + 1 | t \in \mathbb{T}\}$) is the set of time points that correspond to the beginning of a month of the NC (OP) demand charge horizon.

C. Traditional EMPC without peak demand tracking

Let the state x represent the SOC of the BESS. At $t \in \mathbb{T}$ with the state $x(t)$, the traditional EMPC formulation without peak demand tracking is given by,

$$\begin{aligned} \min_{u_1, u_2} \quad & \sum_{k=t}^{\tau_{\text{MPC},t}} \mathcal{C}_1(u_1(k), u_2(k)) + \\ & \mathcal{C}_2(\mathbf{u}_1, 0, 0, t, \tau_{\text{MPC},t}), \end{aligned} \quad (6a)$$

$$\text{s.t. } x(k+1) = x(k) - \frac{u_2(k)}{\text{BESS}_{en}} \Delta T, \quad (6b)$$

$$L_f(k) = \text{PV}_f(k) + u_2(k) + u_1(k), \quad (6c)$$

$$-\bar{u}_2 \leq u_2(k) \leq \bar{u}_2, \quad (6d)$$

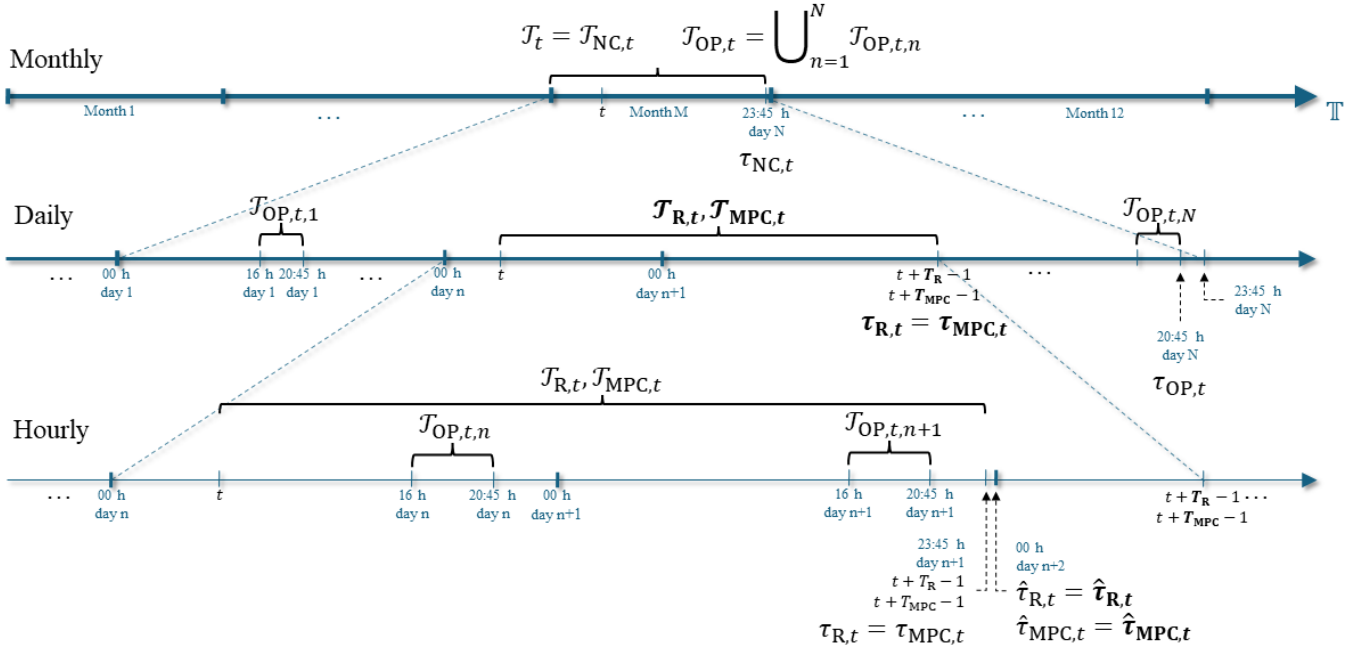


Fig. 2. Temporal schematic example for a 48 h prediction horizon together with a 48 h reference horizon, both starting at time t , which falls on day n of a month M with N days. The set of time points for the month M is denoted by \mathcal{T}_t , with $\mathcal{T}_{NC,t}$ and $\mathcal{T}_{OP,t}$ defining the subsets corresponding to NC and OP demand charge periods, respectively. The final time points for these periods are represented as $\tau_{NC,t}$ and $\tau_{OP,t}$. The set $\mathcal{T}_{OP,t}$ is the union of the daily subset of OP demand charge time points $\mathcal{T}_{OP,t,n}$. Starting from t , the set of all time points in the reference horizon of length T_R are defined in $\mathcal{T}_{R,t}$, with its final time point called $\tau_{R,t}$ and $\hat{\tau}_{R,t}$ marking the time point at which the 50% SOC low threshold is placed. Similarly, the prediction horizon starting at the time point t , with length T_{MPC} , is represented by $\mathcal{T}_{MPC,t}$. The final time point in this horizon is $\tau_{MPC,t}$, and $\hat{\tau}_{MPC,t}$ identifies the time point at which the 50% SOC low threshold is placed. Bold and unbold time parameters $\tau_{MPC,t}$, $\tau_{R,t}$, $\tau_{MPC,t}$, T_R , $\tau_{MPC,t}$, $\tau_{R,t}$, $\hat{\tau}_{MPC,t}$, and $\hat{\tau}_{R,t}$ designate rolling and shrinking horizons, respectively.

$$\underline{x} \leq x(k) \leq \bar{x}, \quad (6e)$$

$$\forall k \in \mathcal{T}_{MPC,t},$$

$$x(\hat{\tau}_{MPC,t}) \geq 0.5. \quad (6f)$$

where k is used to denote the prediction horizon $\mathcal{T}_{MPC,t} = \{t, \dots, \tau_{MPC,t}\}$. Fig. 2 shows the corresponding prediction horizon temporal scheme. The objective function (6a) minimizes the total energy cost and the demand charges assessed over the prediction horizon of length T_{MPC} . The constraint (6b) is the state update equation for the SOC x , where BESS_{en} is the BESS energy capacity. Constraint (6c) is the load balance equation, which ensures that the MG satisfies the forecasted load, L_f . PV_f is the forecasted PV generation. Constraints (6d) and (6e) represent BESS power limits and SOC limits, where \bar{u}_2 is the BESS power capacity and \bar{x} and \underline{x} are the maximum and minimum SOC limits. Constraint (6f) defines a 50% SOC low threshold to be satisfied at time $\hat{\tau}_{MPC,t}$.

Note that BESS losses when $\eta < 1$ are considered only in (1). The load balance in (6c) and the state update in (6b) assume the BESS is 100% efficient, as in [15], [21], to maintain convexity. The work presented in [21] implements a traditional EMPC without peak demand tracking.

The MG model presented above has minor shortcomings that are important to address for future implementations. First, the model does not restrict the power imported from the grid, which can be addressed as an upper (and lower) limit constraint on u_1 . Second, assigning different energy rates for power imported from and exported to the grid represents another improvement, which can be achieved by incorporating

separate energy cost terms for positive and negative values of u_1 in (1). Finally, the model does not account for fossil fuel generation units, which could be included by adding their quadratic cost to the objective function.

D. Traditional EMPC with peak demand tracking

The traditional EMPC presented above can also include memory of the previously achieved peaks by incorporating $\hat{P}_{NC}(t)$ and $\hat{P}_{OP}(t)$ from (3a) and (3b) into \mathcal{C}_2 . At $t \in \mathbb{T}$ with the state $x(t)$, the resulting traditional EMPC algorithm with peak demand tracking is defined as,

$$\begin{aligned} \min_{u_1, u_2} \quad & \sum_{k=t}^{\tau_{MPC,t}} \mathcal{C}_1(u_1(k), u_2(k)) + \\ & \mathcal{C}_2(\mathbf{u}_1, \hat{P}_{NC}(t), \hat{P}_{OP}(t), t, \tau_{MPC,t}), \quad (7) \\ \text{s.t.} \quad & (6b), (6c), (6d), (6e), \\ & \forall k \in \mathcal{T}_{MPC,t}, \\ & (6f). \end{aligned}$$

E. SOC low threshold

The timescale mismatch between the monthly demand charge billing cycle and the real-world prediction horizon length of 24 to 48 h requires the addition of a SOC regulation constraint, which is implemented as a 50% SOC low threshold. This constraint ensures that the BESS has sufficient energy at the beginning of each day as the actual monthly peak demand could occur on any day of the month. The SOC low threshold

at the beginning of each day would not be needed if the prediction horizon spanned the entire month. In that case, the SOC would be allowed to reach any value at the end of each day to minimize monthly peak demands.

However, enforcing the SOC low threshold limits the BESS flexibility within the prediction horizon. For example, when the prediction horizon is 24 h, the SOC low threshold will be placed at most 24 h ahead. Lesser BESS flexibility will be available for peak demand reduction within the prediction horizon when compared to cases without a low threshold. Therefore, where the end of the prediction horizon is defined, and where the 50% SOC low threshold is placed, play a crucial role in the BESS flexibility to reduce demand charges. The 50% SOC low threshold could also ensure that the BESS has sufficient energy to balance forecast errors. Forecast errors are not considered in this work and will be explored in a future publication.

We consider two approaches for the prediction horizon length and the placement of the 50% SOC low threshold: shrinking and rolling prediction horizon. Shrinking the prediction horizon implies that the final time point of the prediction horizon, $\tau_{\text{MPC},t}$, is fixed at the end of a day and it does not advance forward to the next day. This means that $\tau_{\text{MPC},t}$ is defined at the beginning of the day and remains fixed until t advances to the next day. Also, the 50% SOC low threshold is placed at the end of the prediction horizon, i.e., $\hat{\tau}_{\text{MPC},t} = \tau_{\text{MPC},t} + 1$.

On the other hand, the horizon length is kept constant for rolling prediction horizons such that the last horizon time point advances at every MPC step, and thus $\tau_{\text{MPC},t}$ changes at every MPC step. Under the rolling prediction horizon, the 50% SOC low threshold is placed at the last midnight time point included in the prediction horizon and moves to midnight of the next day when t advances to the next day. Under this setting, the 50% SOC low threshold will not prevent the BESS from being fully discharged at time points after the constraint, but it will still limit BESS operation during earlier time points within the prediction horizon.

F. Proposed EMPC

1) *MPC Stage:* In the MPC stage of the proposed EMPC algorithm, the mathematical formulation developed by [25] is adapted to incorporate both demand charges (NC and OP) and the online reference trajectory. First, the system model is augmented with two auxiliary state variables, y_{NC} and y_{OP} , to track the two demand charge peaks within the prediction horizon $\mathcal{T}_{\text{MPC},t}$ starting at time t and denoted using \hat{k} . The temporal scheme of the prediction horizon is shown in Fig. 2. The variables y_{NC} and y_{OP} are defined as,

$$y_{\text{NC}}(k+1) = \max\{(1 - \sigma_{\text{NC}}(k))y_{\text{NC}}(k), u_1(k)\}, \quad (8a)$$

$$y_{\text{OP}}(k+1) = \begin{cases} \max\{(1 - \sigma_{\text{OP}}(k))y_{\text{OP}}(k), u_1(k)\} \\ \text{if } k \in \mathcal{T}_{\text{OP},t} \\ \max\{(1 - \sigma_{\text{OP}}(k))y_{\text{OP}}(k), 0\} \\ \text{otherwise,} \end{cases} \quad (8b)$$

for $k > t$, and where σ_{NC} and σ_{OP} are used to reset y_{NC} and y_{OP} at the beginning of each month. y_{OP} is defined as

a piecewise function because it only considers demand values u_1 registered during the OP demand charge set $\mathcal{T}_{\text{OP},t}$, which is disconnected. Both auxiliary variables are initialized at the start of the prediction horizon ($k = t$) with the previously observed peaks ($\hat{P}_{\text{NC}}(t)$ and $\hat{P}_{\text{OP}}(t)$) up to t . Specifically,

$$y_{\text{NC}}(t) = \hat{P}_{\text{NC}}(t), \quad y_{\text{OP}}(t) = \hat{P}_{\text{OP}}(t). \quad (9)$$

The cost function consists of a stage cost and a terminal cost. The stage cost accounts for the energy cost and the demand charges incurred at the end of the month. Denoting $z(k) = (x(k), y_{\text{NC}}(k), y_{\text{OP}}(k))^{\top}$, the stage cost is defined as,

$$L(z(k), u_1(k), u_2(k), k) = \mathcal{C}_1(u_1(k), u_2(k)) + R_{\text{NC}}\sigma_{\text{NC}}(k)y_{\text{NC}}(k) + R_{\text{OP}}\sigma_{\text{OP}}(k)y_{\text{OP}}(k), \quad (10)$$

where the second and third terms correspond to the demand charge costs and are added to the stage cost only when the end of the month is within the prediction horizon, that is, when any time point in \mathbb{T}_{NC} or \mathbb{T}_{OP} belongs to $\mathcal{T}_{\text{MPC},t}$.

The terminal cost uses the reference trajectory to account for demand charges of time points that correspond to a month whose final time point is not within the prediction horizon. Let $z_r(k') = (x_r(k'), u_{r1}(k'), u_{r2}(k'))$ be the reference trajectory over the reference horizon $\mathcal{T}_{\text{R},t}$, which is denoted using \hat{k}' and starts at time $k' = t$. Then, for each $k \in \mathcal{T}_{\text{MPC},t} \cup \{\tau_{\text{MPC},t} + 1\}$, we define the reference trajectory peaks as follows,

$$\hat{y}_{\text{NC}}(k, \hat{k}) = \max_{k' \in \mathcal{T}_{\text{NC},k-1} \cap \mathcal{T}_{\text{R},\hat{k}}} \{u_{r1}(k'), \hat{P}_{\text{NC}}(\hat{k})\}, \quad (11a)$$

$$\check{y}_{\text{NC}}(k, \hat{k}) = (1 - \sigma_{\text{NC}}(k)) \max_{k' \in \mathcal{T}_{\text{NC},k} \cap \mathcal{T}_{\text{R},\hat{k}}, k' \geq k} u_{r1}(k'), \quad (11b)$$

$$\hat{y}_{\text{OP}}(k, \hat{k}) = \max_{k' \in \mathcal{T}_{\text{OP},k-1} \cap \mathcal{T}_{\text{R},\hat{k}}} \{u_{r1}(k'), \hat{P}_{\text{OP}}(\hat{k})\}, \quad (11c)$$

$$\check{y}_{\text{OP}}(k, \hat{k}) = (1 - \sigma_{\text{OP}}(k)) \max_{k' \in \mathcal{T}_{\text{OP},k} \cap \mathcal{T}_{\text{R},\hat{k}}, k' \geq k} u_{r1}(k'), \quad (11d)$$

where $\hat{y}_{\text{NC}}(k, \hat{k})$ ($\hat{y}_{\text{OP}}(k, \hat{k})$) is the maximum of the peak power imported from the grid estimated by the reference trajectory, the u_{r1} peak, for NC (OP) time points and the u_1 peak until time \hat{k} for NC (OP) time points, which is stored in $\hat{P}_{\text{NC}}(\hat{k})$ ($\hat{P}_{\text{OP}}(\hat{k})$). \hat{k} is the time point where the reference trajectory was computed, with $\hat{k} < k$. Furthermore, the time shift in 11a (11c) allows $\hat{y}_{\text{NC}}(k, \hat{k})$ ($\hat{y}_{\text{OP}}(k, \hat{k})$) to compute the peak for the demand charge period just ended, that is, when $k \in \mathbb{T}_{\text{NC}}$ ($k \in \mathbb{T}_{\text{OP}}$) as explained in [25]. $\check{y}_{\text{NC}}(k, \hat{k})$ ($\check{y}_{\text{OP}}(k, \hat{k})$) corresponds to the u_{r1} peak for the NC (OP) time points within $\mathcal{T}_{\text{R},\hat{k}}$ but only after the time point k . Given that the set $\mathcal{T}_{\text{OP},k}$ is disconnected, whenever $\mathcal{T}_{\text{OP},k} \cap \mathcal{T}_{\text{R},\hat{k}}$ is an empty set in shrinking horizon cases, a value of zero is assigned as the maximum of u_{r1} .

In contrast with [25], where the reference horizon starts at the beginning of the month and the reference trajectory is generated in one shot for the entire month, in this work the reference trajectory $\mathcal{T}_{\text{R},\hat{k}}$ is updated at every MPC step, beginning at time \hat{k} and generated for a shorter horizon. Furthermore, the original reference trajectory peak formulations from [25] were accordingly adapted in (11) to incorporate the online reference trajectory proposed.

The terminal cost is then defined as,

$$V_f(z(k), k, \hat{k}) = \quad (12)$$

$$R_{\text{NC}}(\max\{y_{\text{NC}}(k), \check{y}_{\text{NC}}(k, \hat{k})\} - \hat{y}_{\text{NC}}(k, \hat{k})) +$$

$$R_{\text{OP}}(\max\{y_{\text{OP}}(k), \check{y}_{\text{OP}}(k, \hat{k})\} - \hat{y}_{\text{OP}}(k, \hat{k})).$$

With (12) as the terminal cost, there is no incentive to reduce any of the peak demands below the peak predicted by the reference trajectory for time points beyond k . This is because at each time point k a minimum value for the NC (OP) peak is defined by $\check{y}_{\text{NC}}(k, \hat{k})$ ($\check{y}_{\text{OP}}(k, \hat{k})$). In addition, when the end of the demand charge horizon is not included within the prediction horizon starting at \hat{k} , (12) penalizes increments in the peak NC (OP) demand charge $y_{\text{NC}}(k)$ ($y_{\text{OP}}(k)$) for $y_{\text{NC}}(k) > \check{y}_{\text{NC}}(k, \hat{k})$ ($y_{\text{OP}}(k) > \check{y}_{\text{OP}}(k, \hat{k})$) only by the excess amount with respect to $\hat{y}_{\text{NC}}(k, \hat{k})$ ($\hat{y}_{\text{OP}}(k, \hat{k})$).

The formulation developed by [25] also proposes a terminal constraint for the state x based on the reference trajectory as,

$$x(\tau_{\text{MPC},t} + 1) = x_r(\tau_{\text{MPC},t} + 1). \quad (13)$$

Finally, the MPC stage of the proposed EMPC is defined at $t \in \mathbb{T}$ with the state $x(t)$ by,

$$\min_{u_1, u_2} \sum_{k=t}^{\tau_{\text{MPC},t}} L(z(k), u_1(k), u_2(k), k) + \quad (14)$$

$$V_f(z(\tau_{\text{MPC},t} + 1), \tau_{\text{MPC},t} + 1, t),$$

s.t. (6b), (6c), (6d), (6e), (8a), (8b),

$$\forall k \in \mathcal{T}_{\text{MPC},t},$$

$$(9), (13).$$

Beside t , the terminal cost function V_f in (14) is evaluated using the states variables at time $\tau_{\text{MPC},t} + 1$ and at that time point itself. This is done to incorporate demand charge costs into the formulation when the prediction horizon $\mathcal{T}_{\text{MPC},t}$ ends before the demand charge horizon, as the stage cost L does not incorporate demand charges in such cases. In addition, it is important to note that all variables needed to compute $V_f(z(\tau_{\text{MPC},t} + 1), \tau_{\text{MPC},t} + 1, t)$ can be determined either from the reference trajectory $z_r(k') = (x_r(k'), u_{r1}(k'), u_{r2}(k'))$ (computed in advance) or from data collected within the prediction horizon $\mathcal{T}_{\text{MPC},t}$. The only exception occurs when the reference and prediction horizons are of equal length, in which case \check{y}_{NC} and \check{y}_{OP} cannot be computed. In such instances, the values computed by (11) at the previous time point $\tau_{R,t}$ are reused for the subsequent time point $\tau_{R,t} + 1$.

While the optimization in (14) will be also solved in shrinking and rolling horizon fashions, the traditional EMPC and the proposed EMPC differ in how they handle the SOC at the end of the prediction horizon $\mathcal{T}_{\text{MPC},t}$. The traditional EMPC algorithm implements a 50% low SOC threshold at the time step $\hat{\tau}_{\text{MPC},t}$ given by (6f), which corresponds to the terminal SOC constraint for shrinking horizons. The MPC stage of the proposed EMPC in (14) does not include the 50% SOC low threshold as a constraint but the low threshold is instead enforced through the reference trajectory for both shrinking and rolling prediction horizons. The reference trajectory is an input to the MPC stage, and it is obtained by solving

an optimization problem that includes the 50% SOC low threshold constraint as discussed next.

2) *Reference Trajectory without Peak Demand Tracking (Reference Stage)*: The reference trajectory $z_r(k')$ is computed at the reference stage of the proposed EMPC. Its temporal alignment is shown in Fig. 2. The reference trajectory is an input to the MPC stage and is used as a basis for measuring the economic performance of the system. The reference trajectory without peak demand tracking is the sequence $\{(x_r(k'), u_{r1}(k'), u_{r2}(k'))\}_{k' \in \mathcal{T}_{R,t}}$ that solves the following optimization problem over the reference horizon $\mathcal{T}_{R,t}$,

$$\min_{u_{r1}, u_{r2}} \sum_{k'=t}^{\tau_{R,t}} \mathcal{C}_1(u_{r1}(k'), u_{r2}(k')) + \quad (15a)$$

$$\mathcal{C}_2(\mathbf{u}_{r1}, 0, 0, t, \tau_{R,t}),$$

$$\text{s.t. } x_r(k' + 1) = x_r(k') - \frac{u_{r1}(k')}{\text{BESS}_{en}} \Delta T, \quad (15b)$$

$$L_f(k') = \text{PV}_f(k') + u_{r2}(k') + u_{r1}(k'), \quad (15c)$$

$$\underline{u}_2 \leq u_{r2}(k') \leq \bar{u}_2, \quad (15d)$$

$$\underline{x} \leq x_r(k') \leq \bar{x}, \quad (15e)$$

$$\forall k' \in \mathcal{T}_{R,t},$$

$$x_r(t) = x(t), \quad (15f)$$

$$x_r(\hat{\tau}_{R,t}) \geq 0.5, \quad (15g)$$

where $\hat{\tau}_{R,t}$ is the time point where the 50% SOC low threshold is placed, and \mathbf{u}_{r1} is a vector where each element corresponds to $u_{r1}(t)$ for all $t \in \mathbb{T}$. Similar to the prediction horizons described above, the reference horizon can be shrinking or rolling. The constraint (15g) is placed at the end of the shrinking reference horizon ($\hat{\tau}_{R,t} = \tau_{R,t} + 1$), while for the rolling reference horizon, the constraint (15g) is assigned to the last midnight time point within the reference horizon ($\hat{\tau}_{R,t} \leq \tau_{R,t}$).

3) *Reference Trajectory with Peak Demand Tracking (Reference Stage)*: A reference trajectory that incorporates previous peak demands is the control sequence $\{(x_r(k'), u_{r1}(k'), u_{r2}(k'))\}_{k' \in \mathcal{T}_{R,t}}$ that solves the following optimization problem,

$$\min_{u_{r1}, u_{r2}} \sum_{k'=t}^{\tau_{R,t}} \mathcal{C}_1(u_{r1}(k'), u_{r2}(k')) + \quad (16)$$

$$\mathcal{C}_2(\mathbf{u}_{r1}, \hat{P}_{\text{NC}}(t), \hat{P}_{\text{OP}}(t), t, \tau_{R,t}),$$

$$\text{s.t. } (15b), (15c), (15d), (15e),$$

$$\forall k' \in \mathcal{T}_{R,t},$$

$$(15f), (15g),$$

where compared to (15), $\hat{P}_{\text{NC}}(t)$ and $\hat{P}_{\text{OP}}(t)$ have been included in \mathcal{C}_2 when computing demand charges in the objective function. Given the much shorter reference horizon (24-48 h) than the demand charge horizon (one month), a new reference trajectory is generated at every MPC step.

As was explained in Section II-A, we refer to MPC horizon as the prediction horizon. Additionally, note that the reference trajectory is a set of feasible states and control actions, and the reference horizon $\mathcal{T}_{R,t}$ and the prediction horizon $\mathcal{T}_{\text{MPC},t}$ define different sets of time points.

The implementation of the proposed EMPC considering a reference trajectory with peak demand tracking is summarized in Algorithm 1. The proposed EMPC considering a reference trajectory without peak demand tracking can also be summarized in Algorithm 1, but problem (15) will be solved in line 11 instead of problem (16).

Algorithm 1 Proposed EMPC with Peak Tracking

- 1: Initialize $x(0)$.
 - 2: **for** $t \in \mathbb{T}$ **do**
 - 3: **if** $t \in \mathbb{T}_{\text{NC}}$ **then**
 - 4: Define the time set for the month \mathcal{T}_t ;
 - 5: Define the subsets corresponding to NC and OP demand charge periods $\mathcal{T}_{\text{NC},t}$ and $\mathcal{T}_{\text{OP},t}$;
 - 6: Assign the final time points $\tau_{\text{NC},t}$ and $\tau_{\text{OP},t}$ of the subsets $\mathcal{T}_{\text{NC},t}$ and $\mathcal{T}_{\text{OP},t}$.
 - 7: **end if**
 - 8: **Reference stage**
 - 9: Observe system current state $x(t)$, and monthly peak tracking variables $\hat{P}_{\text{NC}}(t)$ and $\hat{P}_{\text{OP}}(t)$;
 - 10: Define the reference horizon time set $\mathcal{T}_{\text{R},t}$, and assign its final time point $\tau_{\text{R},t}$ and the time point where the SOC low threshold is placed $\hat{\tau}_{\text{R},t}$;
 - 11: Forecast load $\{L_f(k')\}_{k' \in \mathcal{T}_{\text{R},t}}$ and PV generation $\{PV_f(k')\}_{k' \in \mathcal{T}_{\text{R},t}}$ over the reference horizon;
 - 12: Solve the problem (16) to obtain the reference trajectory $\{x_r(k'), u_{r1}(k'), u_{r2}(k')\}_{k' \in \mathcal{T}_{\text{R},t}}$;
 - 13: **MPC stage**
 - 14: Define prediction horizon time set $\mathcal{T}_{\text{MPC},t}$, and assign its final time point $\tau_{\text{MPC},t}$ and the time point where the SOC low threshold is placed $\hat{\tau}_{\text{MPC},t}$;
 - 15: Forecast load $\{L_f(k)\}_{k \in \mathcal{T}_{\text{MPC},t}}$ and PV generation $\{PV_f(k)\}_{k \in \mathcal{T}_{\text{MPC},t}}$ over the prediction horizon;
 - 16: Compute the peaks of the reference trajectory $\hat{y}_{\text{NC}}(k, \hat{k})$, $\check{y}_{\text{NC}}(k, \hat{k})$, $\hat{y}_{\text{OP}}(k, \hat{k})$ and $\check{y}_{\text{OP}}(k, \hat{k})$ according to (11) with $\hat{k} = t$ and $t = \tau_{\text{MPC},t} + 1$;
 - 17: Observe system current state $x(t)$, peaks of the reference trajectory $(\hat{y}_{\text{NC}}(\tau_{\text{MPC},t} + 1, t), \check{y}_{\text{NC}}(\tau_{\text{MPC},t} + 1, t), \hat{y}_{\text{OP}}(\tau_{\text{MPC},t} + 1, t), \check{y}_{\text{OP}}(\tau_{\text{MPC},t} + 1, t))$, and monthly peak tracking variables $\hat{P}_{\text{NC}}(t)$ and $\hat{P}_{\text{OP}}(t)$;
 - 18: Solve the problem (14) to obtain the optimal control $\{x(k), u_1(k), u_2(k)\}_{k \in \mathcal{T}_{\text{MPC},t}}$ over the prediction horizon;
 - 19: Save $x(t+1)$, $u_1(t)$, and $u_2(t)$;
 - 20: Update monthly peak tracking variables $\hat{P}_{\text{NC}}(t+1)$ and $\hat{P}_{\text{OP}}(t+1)$ according to (3a) and (3b).
 - 21: **end for**
-

III. CASE STUDY

A. Microgrid at the Port of San Diego

The MG at the Port of San Diego (latitude 32.69° , longitude -117.14°) consists of a 700 kW PV plant and a BESS system. The BESS has an energy capacity $\text{BESS}_{\text{en}} = 2,500$ kWh and power capacity $\bar{u}_2 = 700$ kW. The BESS charging/discharging efficiency (η) is 80%, and the maximum (\bar{x}) and minimum (\underline{x}) SOC limits the BESS is allowed to reach are 0.8 and

0.2, respectively. The electricity cost of the MG considers a constant energy rate (R_{EC}) of \$0.1/kWh, and NC and OP demand charge rates (R_{NC} and R_{OP}) of \$24.48/kWh and \$19.19/kWh, respectively. These are non-residential rates from 2020 (SDG&E AL-TOU tariff) [29]. R_{OP} (R_{EC}) is the average between the winter and summer OP demand charge (Off-Peak energy) rates. While energy rates vary in practice, for example based on time-of-use, the interpretation of the demand charge results is simplified through a constant R_{EC} . Our proposed EMPC approach is generalizable to variable energy rates.

The PV panel tilt is 5° , and the entire PV array faces southwest at an azimuth angle of 219° from north. PV output is obtained from the System Advisor Model (SAM) [30] for the year 2019. The solar resource is estimated using a 30 minute resolution dataset from the National Solar Radiation Database (NSRDB) and interpolated to obtain a time series with 15 min resolution.

Real 15 min resolution load data provided by the Port of San Diego for 2019 is utilized. On most days, the peak load occurs at night, as a large share of the load is from lighting. There is no significant difference in load profiles between weekends and weekdays.

MG optimization case studies are carried out using CVX, a package for solving convex programs in the MATLAB environment [31]. The simulation time step (ΔT) was chosen as 15 min, and the initial SOC value $x(0)$ for January 1 is chosen as 0.5. Finally, perfect forecasts are assumed for load and PV generation.

B. Case setup

In Section IV, the proposed EMPC (noted as ‘‘EMPC’’) is compared with traditional EMPC (noted as ‘‘Trad’’) considering different receding manners, horizon lengths, and peak tracking setups:

1) *Shrinking and rolling horizons*: For the shrinking horizon manner, the horizon length shrinks one time point each MPC step and gets restarted daily, while for the rolling horizon manner, the horizon length remains constant, with the forecast updated each MPC step for both cases. Each receding manner implements the 50% SOC low threshold and the terminal SOC constraint differently, which leads to distinct BESS flexibility. Details of SOC constraint implementation for Trad and EMPC with shrinking and rolling horizons are explained separately.

First, the 50% SOC low threshold is set at the end of the current day. For the shrinking horizon manner, it is at the end of the prediction horizon and the end of the reference horizon for Trad (6f) and EMPC (15g), respectively. On the other hand, for the rolling horizon manner, the 50% SOC low threshold constraint stays at the same time point when the rolling horizon moves forward in time. Then, the 50% SOC low threshold gets closer to the beginning of the prediction horizon and the reference horizon for Trad and EMPC, respectively.

Secondly, as EMPC has two stages (the first reference stage that includes placing the 50% SOC low threshold, and the second MPC stage that includes placing the terminal SOC constraint), the shrinking and rolling horizon manners further

impact the BESS performance. For EMPC to track the reference trajectory, following the 50% SOC low threshold placed in the first reference stage, a terminal SOC constraint (13) is set at the end of the prediction horizon during the MPC stage. For the shrinking horizon manner, the terminal SOC constraint overlaps with the 50% SOC low threshold (15g) when the reference horizon and the prediction horizon have the same length. On the other hand, with rolling horizon, the terminal SOC constraint (13) is placed at the end of the prediction horizon, which extends beyond the time point where the 50% SOC low threshold is placed.

In summary, for EMPC with shrinking horizon, the 50% SOC low threshold is enforced at the end of the prediction horizon during the MPC stage for all shrinking horizon cases (except for the case with 48 h reference horizon and 24 h prediction horizon), while for EMPC with rolling horizon, more BESS discharging can occur before the terminal SOC constraint (13) becomes active.

2) *24 and 48 h reference and prediction horizons:* For both receding manners, the results for both Trad and EMPC strategies are presented considering 24 and 48 h prediction horizons. In addition, the EMPC strategy considers 24 and 48 h reference horizons when the prediction horizon is 24 h, and it considers a 48 h reference horizon when the prediction horizon is 48 h.

3) *Peak tracking:* For both receding manners, both Trad and EMPC for all horizon lengths are constructed with (“WT”) and without (“NT”) peak demand tracking.

4) *Results section outline:* In total, 20 cases are demonstrated in the next Section. Specifically, 10 cases with shrinking horizons are discussed in Section IV-A and Table I, and the other 10 cases with rolling horizons are discussed in Section IV-B and Table II. Furthermore, an ideal EMPC case with a 24 h prediction horizon and a full-month reference trajectory with perfect forecast (noted as EMPC*) is shown in Tables I and II. EMPC* is an ideal case since information to generate a full-month reference trajectory is generally not available. However, EMPC* provides the best performance that can be achieved in this case study. The control actions obtained from EMPC* are cost-optimal since the reference horizon in EMPC* spans the entire month.

IV. RESULTS AND DISCUSSION

A. Shrinking-horizon cases

1) *Full month reference horizon:* In this section, the ideal case, EMPC*, is compared with Trad and EMPC for shrinking horizon cases with the monthly BESS SOC analysis. While Trad with a shrinking horizon uses the 50% SOC low threshold as the terminal SOC constraint, EMPC with a shrinking horizon overlaps the 50% SOC low threshold with the terminal SOC constraint when the reference horizon and the prediction horizon have the same length. EMPC* places the 50% SOC low threshold at the end of the reference horizon, which corresponds to the full month. While the 50% SOC

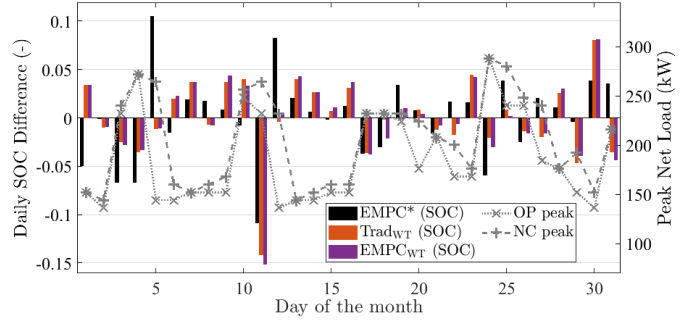


Fig. 3. Daily SOC difference between final and initial SOC (colored bars) together with daily NC peak (dashed gray line with “+” markers) and OP peak net loads (dotted gray line with “x” markers) in March 2019 for EMPC* and the following shrinking horizon cases: Trad_{WT} with $T_{MPC} = 48$ h, and EMPC_{WT} with $T_R = T_{MPC} = 48$ h. Cases with $T_{MPC} = 24$ h have daily SOC difference equals zero because SOC starts and ends at 50% every day.

low threshold guarantees that the BESS always has capacity available for cost minimization the next day, which is outside the prediction horizon, the 50% SOC low threshold as a terminal SOC constraint limits the BESS energy allocation flexibility at the end of each prediction horizon.

The effect of the terminal SOC constraint on the demand charge reduction for all cases is further explained using the daily SOC difference between hours 00 and 24 in Fig. 3. In March 2019, Fig. 3 shows that larger daily SOC differences are observed for EMPC* compared to the other cases. Furthermore, large changes from negative SOC difference to positive SOC difference on consecutive days coincide with large drops in OP peak net load. For example, the SOC difference increases from -0.06 on day 4 to 0.1 on day 5 as a result of the daily OP peak net load decreasing from 275 kW to 175 kW. Similar trends are observed on days 10, 11, and 24. With perfect knowledge of a full-month reference trajectory, EMPC* is able to adjust the SOC freely and allocate more energy on days with higher peak net load to reduce OP demand charges.

2) *24-hour reference and prediction horizons:* In this section EMPC is compared with Trad under the simplest settings-24 h, NT. EMPC_{NT} outperforms the benchmark case, Trad_{NT}, with a lower annual cost (Table I). Even though the reference trajectory in EMPC_{NT} does not track the peak, in (9) EMPC includes information on the highest peaks up to time t in the auxiliary variables y_{NC} and y_{OP} . Thus, EMPC_{NT} has the peak information from a peak tracking method embedded within the formulation. When the highest monthly peak observed till time t is higher than the predicted demand, compared to Trad_{NT}, EMPC_{NT} dispatches the BESS less aggressively for demand charge reduction, reducing the BESS loss cost.

For example, from 18:30 h to 21:00 h on March 24, 2019 (Fig. 4), Trad_{NT} (blue line) dispatches the BESS aggressively for OP demand reduction, while EMPC_{NT} (yellow line) allows more OP demand while remaining below the previous highest OP demand (Fig. 4a). Compared to Trad_{NT}, EMPC_{NT} controls the BESS less aggressively (Fig. 4b), maintaining the SOC close to 50%, resulting in lower BESS losses.

On the other hand, reduced BESS charging in EMPC causes issues when a high net load exists close to the end of the day.

TABLE I
ANNUAL COST COMPONENTS FOR EMPC* AND SHRINKING PREDICTION HORIZON CASES FOR THE YEAR 2019. THE HIGHEST AND THE LOWEST ANNUAL COSTS ARE HIGHLIGHTED IN RED AND BOLD, RESPECTIVELY.

Cases	EMPC*	Trad _{NT}	Trad _{WT}	EMPC _{NT}	EMPC _{WT}	Trad _{NT}	Trad _{WT}	EMPC _{NT}	EMPC _{WT}	EMPC _{NT}	EMPC _{WT}
Run time (s)	-	0.7	0.7	1.4	1.4	1.0	1.0	1.5	1.5	3.1	3.1
T_{MPC}	24 h	24 h	24 h	24 h	24 h	48 h	48 h	24 h	24 h	48 h	48 h
T_R	1 mo	-	-	24 h	24 h	-	-	48 h	48 h	48 h	48 h
NCDC (k\$)	43.0	51.7	39.5	58.9	39.5	46.3	38.2	53.9	38.2	46.5	38.2
OPDC (k\$)	1.7	23.1	19.3	18.0	19.3	22.1	19.1	17.4	19.1	18.4	19.1
Energy Cost (k\$)	14.4	14.4	14.4	14.4	14.4	14.4	14.4	14.4	14.4	14.4	14.4
BESS loss (k\$)	5.5	10.0	4.9	3.3	4.9	9.0	5.0	4.9	5.0	4.1	5.0
Annual Cost (k\$)	64.6	99.2	78.1	94.5	78.1	91.8	76.7	90.6	76.7	83.3	76.7

Compared to Trad_{NT}, EMPC_{NT} has less BESS energy left that can be dispatched to reduce the NC peak. This results in a higher annual NCDC as shown in Table I (NCDC = k\$58.9 vs. k\$51.7). For example, in Fig. 4b the low SOC at 21:00 h and the terminal SOC constraint causes EMPC_{NT} to reach a NC peak of 238 kW compared to the Trad_{NT} peak of 221 kW. This higher NC demand close to the end of the day is observed in all EMPC cases throughout the year because the Port of San Diego consists of mostly unconditioned warehouses and outdoor lighting that trigger a higher net load after 21:00 h.

Adding peak tracking to both control strategies, Trad_{WT} and EMPC_{WT} yield the same annual cost of k\$78.1 (Table I).

3) *Longer reference and prediction horizons:* Similar trends are observed for the 48 h horizons: without peak tracking, EMPC_{NT} with $T_R = T_{MPC} = 48$ h outperforms Trad_{NT} with $T_{MPC} = 48$ h by k\$8.5 (= k\$91.8 – k\$83.3); and with peak tracking, EMPC_{WT} with $T_R = T_{MPC} = 48$ h and Trad_{WT} with $T_{MPC} = 48$ h have the same annual cost of k\$76.7.

The higher NCDC observed in EMPC_{NT} compared to Trad_{NT} in the previous section due to the terminal SOC constraint and reduced BESS charging can be mitigated by expanding both the prediction horizon and the reference horizon. Expanding the reference horizon from 24 h to 48 h reduces the annual NCDC from k\$58.9 to k\$53.5 for EMPC_{NT}, and from k\$39.5 to k\$38.2 for EMPC_{WT}. By further expanding the prediction horizon from 24 h to 48 h, the annual EMPC_{NT} NCDC is reduced from k\$53.9 to k\$46.5. As no terminal SOC constraint is set at the end of the first day, the BESS has more flexibility to allocate its energy for demand charge reduction. The benefit of prediction horizon expansion is also observed for Trad. Yet higher NCDC and lower BESS loss in EMPC_{NT} compared to Trad_{NT} are also observed for the 48 h prediction horizon with NCDC = k\$46.5 versus k\$46.3 and BESS loss = k\$4.1 versus k\$9.0. Besides expanding the horizon, implementing a rolling horizon instead of a shrinking horizon also allows relaxing the terminal SOC constraint, which is further discussed in Section IV-B.

All cases presented in Table I and Table II share the same energy cost (excluding BESS losses), as the charging timing of BESS does not affect the energy cost as the energy rate is constant throughout the day.

B. Rolling-horizon cases

1) *Rolling versus shrinking horizons:* Results for NT with rolling horizons in Table II show that EMPC outperforms Trad

for both 24 h and 48 h horizons, which is consistent with what was observed for the shrinking horizon (Section IV-A). On the other hand, for WT the annual costs between EMPC and Trad differ, which is not the same pattern observed for shrinking horizons. The differences between the shrinking and rolling horizon cases are caused by the difference in the placement of 50% SOC low threshold time point within the reference horizon (Section III-B1). As the end of the prediction horizon shifts away from the 50% SOC low threshold of the reference horizon, more BESS discharging can occur before the terminal SOC constraint (13) becomes active. That is, the BESS is discharged deeper after the 50% SOC low threshold placement to reduce electricity costs, leading to low SOC at the end of the reference horizon, which is then assigned as the terminal SOC constraint by (13) in the prediction horizon. In this case, the reference SOC value used as the terminal SOC constraint in EMPC is close to the minimal SOC limit, \underline{x} .

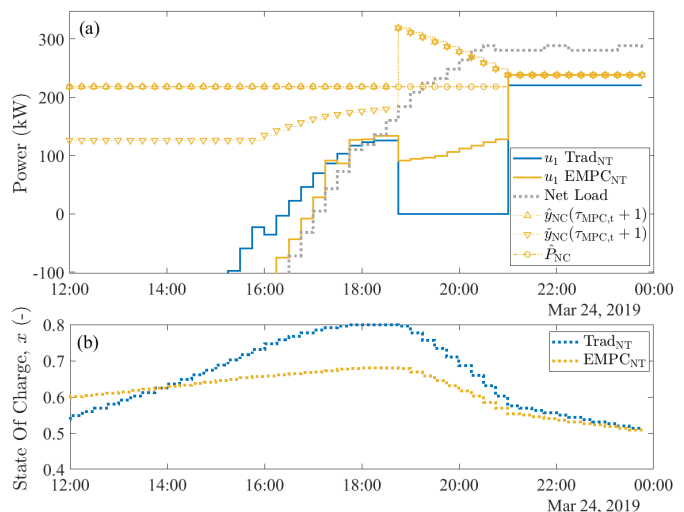


Fig. 4. March 24 timeseries of Trad_{NT} with $T_{MPC} = 24$ h, and EMPC_{NT} with $T_{MPC} = T_R = 24$ h shrinking horizon cases for: (a) demand (u_t , solid lines) together with $\hat{y}_{NC}(\tau_{MPC,t} + 1)$, $\hat{y}_{NC}(\tau_{MPC,t} + 1)$, and $\hat{P}_{NC}(t)$ for EMPC_{NT}; and (b) SOC (x , dotted lines). The dotted gray line in (a) represents the net load, $L_f - PV_f$. The net load before 16:00 h is less than -100 kW due to solar over-generation.

2) *24-hour reference and prediction horizons:* For the 24 h horizons, EMPC_{WT} has a higher annual cost than Trad_{WT} (k\$91.5 versus k\$77.4 in Table II) because of excessive BESS discharges during OP hours that generate larger NC peak demands at night in EMPC_{WT} compared to Trad_{WT}

(NCDC= k\$66.0 versus k\$39.4 in Table II). Indeed, the difference in NCDC corresponds to the largest share of the annual cost for EMPC_{WT} and negates any reduction achieved in OPDC and BESS losses compared to Trad_{WT} . Figure 5 shows the March 24 u_1 timeseries as an example, where EMPC_{WT} shows a lower OP peak demand but a larger NC peak compared to Trad_{WT} (OP peak: 18 kW versus 134 kW, NC peak: 242 kW versus 139 kW, respectively). Figure 5 also shows the difference in SOC between EMPC_{WT} and Trad_{WT} , where the former reaches 30% SOC at 21:00 h while SOC for Trad_{WT} is 67%.

The aggressive BESS discharge during OP hours for EMPC_{WT} are a consequence of the reference trajectory suggesting OP and NC peak demand increments within the prediction horizon. The reference trajectory suggests an NC (OP) peak demand increment within the prediction horizon when $\hat{y}_{\text{NC}}(\tau_{\text{MPC},t} + 1) > \hat{P}_{\text{NC}}(t) > \check{y}_{\text{NC}}(\tau_{\text{MPC},t} + 1)$ ($\hat{y}_{\text{OP}}(\tau_{\text{MPC},t} + 1) > \hat{P}_{\text{OP}}(t) > \check{y}_{\text{OP}}(\tau_{\text{MPC},t} + 1)$). Figure 5 shows that the reference trajectory starts suggesting increments at 14:45 h for OP hours and at 18:30 h for NC hours.

The reference trajectory proposes increments in OP and NC peaks within the prediction horizon because of the proximity of the 50% SOC low threshold to time t in the reference horizon. Indeed, a low SOC as an initial condition for the reference trajectory generates aggressive reference BESS charging at the beginning of the reference horizon, and also aggressive discharging towards the end of the reference horizon. The EMPC algorithm with increments in NC and OP peaks within the prediction horizon as a reference and a low terminal SOC state will aggressively discharge the BESS to avoid peak demand increments within the prediction horizon (and minimize the terminal cost V_f).

3) *Longer reference and prediction horizons*: The explanation provided for the 24 h horizons also applies to EMPC_{WT} with $T_{\text{R}} = T_{\text{MPC}} = 48$ h, but here a 2% reduction in the annual cost is achieved with respect to Trad_{WT} with $T_{\text{MPC}} = 48$ h. The main cost reduction in EMPC_{WT} comes from a lower OPDC (12.6% lower than Trad_{WT}), while NCDC only increases 1.5%, as shown in Table II. The annual cost reduction for the 48 h horizon is a result of BESS discharge during OP hours in EMPC_{WT} that is more moderated than the case of EMPC with 24 h reference horizon but still more aggressive than the Trad_{WT} with $T_{\text{MPC}} = 48$ h. As an example, Fig. 6 shows EMPC_{WT} with an OP peak of 108 kW (NC peak of 143 kW), while an OP peak of 134 kW (NC peak of 134 kW) is obtained with Trad_{WT} . The EMPC_{WT} improvement explained above is not observed with $T_{\text{R}} = 48$ h and $T_{\text{MPC}} = 24$ h because in this case the prediction horizon ends before the 50% SOC low threshold is placed in the reference horizon.

EMPC_{WT} with $T_{\text{R}} = T_{\text{MPC}} = 48$ h implements a more moderated BESS discharge than EMPC_{WT} with $T_{\text{R}} = T_{\text{MPC}} = 24$ h because of the longer reference and prediction horizons. The 48 h reference trajectory avoids suggesting peak demand increments within the EMPC prediction horizon because the 50% threshold is at least 24 h ahead of the reference horizon initial time point at every MPC step. No NC (OP) peak increments within the prediction horizon are suggested by

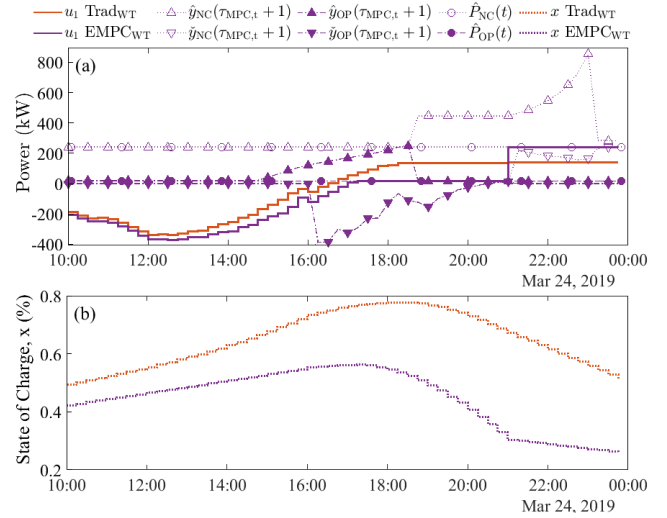


Fig. 5. March 24 timeseries of (a) u_1 , and (b) x , together with $\hat{y}_{\text{NC}}(\tau_{\text{MPC},t} + 1)$, $\check{y}_{\text{NC}}(\tau_{\text{MPC},t} + 1)$, $\hat{y}_{\text{OP}}(\tau_{\text{MPC},t} + 1)$, $\check{y}_{\text{OP}}(\tau_{\text{MPC},t} + 1)$, $\hat{P}_{\text{NC}}(t)$, and $\hat{P}_{\text{OP}}(t)$ for Trad_{WT} with $T_{\text{MPC}} = 24$ h and EMPC_{WT} with $T_{\text{R}} = T_{\text{MPC}} = 24$ h. All results are for rolling horizon cases.

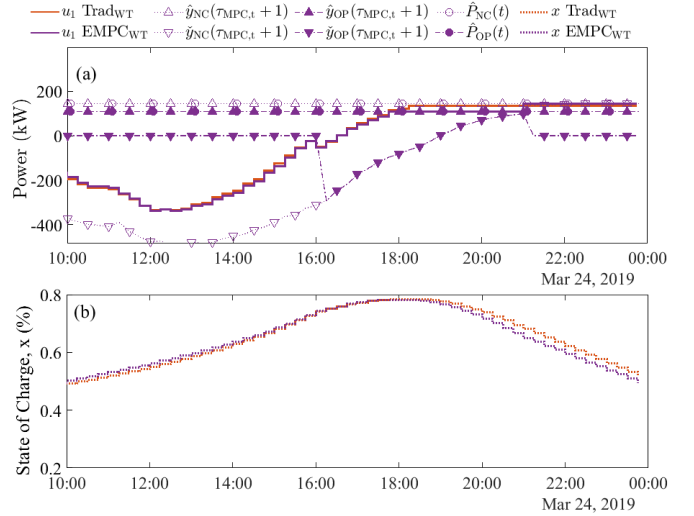


Fig. 6. March 24 timeseries of (a) u_1 , and (b) x , together with $\hat{y}_{\text{NC}}(\tau_{\text{MPC},t} + 1)$, $\check{y}_{\text{NC}}(\tau_{\text{MPC},t} + 1)$, $\hat{y}_{\text{OP}}(\tau_{\text{MPC},t} + 1)$, $\check{y}_{\text{OP}}(\tau_{\text{MPC},t} + 1)$, $\hat{P}_{\text{NC}}(t)$, and $\hat{P}_{\text{OP}}(t)$ for Trad_{WT} with $T_{\text{MPC}} = 48$ h and EMPC_{WT} with $T_{\text{R}} = T_{\text{MPC}} = 48$ h. All results are for rolling horizon cases.

the reference trajectory when $\hat{y}_{\text{NC}}(\tau_{\text{MPC},t} + 1) = \hat{P}_{\text{NC}}(t)$ ($\hat{y}_{\text{OP}}(\tau_{\text{MPC},t} + 1) = \hat{P}_{\text{OP}}(t)$). The 48 h prediction horizon includes two OP time periods with a 19 h gap in between that reduces BESS discharging in the first OP period to keep enough energy for the second OP period. Thus, the 48 h prediction horizon prevents the BESS from reaching low SOC levels at the end of the first OP time period. As an example, Fig. 6 shows EMPC_{WT} with $T_{\text{R}} = T_{\text{MPC}} = 48$ h at a SOC of 65% at 21:00 h, while at the same time a 68% SOC is reached by Trad_{WT} with $T_{\text{MPC}} = 48$ h.

C. Run time comparison and scalability

Table I and Table II shows that the average run time of a single simulation step for EMPC is 1.4 s (3.1 s) for 24 h

TABLE II

ANNUAL COST COMPONENTS FOR EMPC* AND ROLLING PREDICTION HORIZON CASES FOR THE YEAR 2019. THE HIGHEST AND THE LOWEST ANNUAL COSTS ARE HIGHLIGHTED IN RED AND BOLD, RESPECTIVELY.

Cases	EMPC*	Trad _{NT}	Trad _{WT}	EMPC _{NT}	EMPC _{WT}	Trad _{NT}	Trad _{WT}	EMPC _{NT}	EMPC _{WT}	EMPC _{NT}	EMPC _{WT}
Run time (s)	-	0.8	0.8	1.9	1.9	1.1	1.1	2.2	2.2	3.9	3.9
T_{MPC}	24 h	24 h	24 h	24 h	24 h	48 h	48 h	24 h	24 h	48 h	48 h
T_R	1 mo	-	-	24 h	24 h	-	-	48 h	48 h	48 h	48 h
NCDC (k\$)	43.0	53.1	39.4	66.2	66.0	49.3	39.6	47.0	39.5	41.6	40.2
OPDC (k\$)	1.7	21.9	18.4	8.9	7.5	20.3	17.5	18.8	17.5	18.9	15.3
Energy Cost (k\$)	14.4	14.4	14.4	14.4	14.4	14.4	14.4	14.4	14.4	14.4	14.4
BESS loss (k\$)	5.5	9.9	5.1	3.4	3.5	9.0	5.0	4.0	5.0	4.5	5.1
Annual Cost (k\$)	64.6	99.3	77.4	92.9	91.5	92.9	76.5	84.2	76.5	79.5	74.9

(48 h) shrinking reference and prediction horizons, whereas the average run time for Trad is 0.7 s (1.0 s) for the same horizon configurations. For rolling horizons, the average run time is 1.9 s (3.9 s) for EMPC and 0.8 s (1.1 s) for Trad with 24 h (48 h) reference and prediction horizons. Note that a decrease of prediction horizon length, while reducing computational cost for more efficient real-time implementation means that less future information is available for MPC and thus may lead to suboptimal economic performance.

The proposed method in Section II-F requires solving two nominal EMPC problems based on convex optimization (one for the reference trajectory, and another for real-time dispatch) at each simulation step for real-time execution. Convex optimization-based EMPC for systems such as the one proposed in this method has a low computational cost, and a variety of tools (like CVX, YALMIP) are available to get accurate solutions efficiently [32]. The case study in Section III considers one PV system and a BESS in a grid connected microgrid (MG). However, the proposed method can be extended to multiple dispatchable units within a MG or multiple MGs. The only requirement for scaling up the model is the inclusion of additional constraints: equality constraints to capture the state of charge dynamics of BESS systems, and inequality constraints to account for the power ratings of BESS and PV systems. For example, two PV and two BESS systems over a 24 h prediction horizon (with $T_{MPC} = 96$ discrete time steps and $\Delta T = 15$ min) entails adding just T_{MPC} optimization variables (for the second BESS dispatch power) and $3T_{MPC}$ constraints (for the second BESS maximum and minimum charging/discharging power limits and SOC update) for each MPC step, which makes the problem scale linearly. Convex optimization problems involving 1,000 - 10,000s variables and constraints can be reliably solved by standard solvers on a single machine [32], [33]. The low run-time of a single simulation step (corresponding to 15 min in real life) varying between 1.4 - 3.9 s for the different prediction horizons and shrinking/rolling horizon manners in the case study, also serves as a practical reinforcement of the scalability of the proposed method.

D. Recursive feasibility and stability comparison with [25]

In [25, Eq. (2)], the MPC is parametrized by only those initial states that are able to give a feasible control input sequence over the prediction horizon, which enforces recursive feasibility by construction. In our work, as evidenced by (13), the terminal state set for the MPC is equal to the value of the predicted reference state at the time point corresponding to the

terminal time point of the MPC stage. For our case studies, the entire state set (SOC range) from 0.2 to 0.8 can be traversed in about 9 time steps. The prediction horizon varies between 24 to 48 h, which makes the time steps within an MPC prediction horizon vary between 96–192 steps. Thus, recursive feasibility is always attained as long as the prediction horizon is more than 9 time steps, which like [25] is enforced by construction of the optimal control problem in our work.

[25] established that the region of attraction¹ under their control law is nothing other than the feasible initial state set under assumptions of strict dissipativity, stability of the terminal region and a-priori knowledge of the reference trajectory for the entire window for which the demand charge is assessed (i.e., a month). For our work, for both the shrinking and rolling horizon cases, stability (the way it is defined in a classical sense in [25]) with respect to the reference trajectory is an undefined problem and has no useful result, as the reference trajectory changes for each time step for the rolling horizon, and each 24 or 48 h period for the shrinking horizon cases.

V. CONCLUSION AND FUTURE WORK

The proposed EMPC is a more practical implementation of the original formulation developed by [25] for optimal BESS dispatch in a microgrid with variable renewable energy resources to minimize demand charges. The formulation from [25] requires one month forecasts of renewable energy and load to generate the reference trajectory which is generally not available. On the other hand, we test 24 h and 48 h horizons for which forecasts are available in practice. Annual simulations show that even using a reference trajectory that is shorter than the demand charge assessment window, which is updated at every MPC step, the proposed EMPC algorithm still provides a total cost that is equal to (for shrinking horizons) or better than (for rolling horizons) the traditional EMPC when the monthly peak demands are tracked. The only exception is the rolling horizon case with a 24 h reference horizon. For future implementations, the proposed EMPC with peak demand tracking and 48 h prediction and reference rolling horizons is preferred as it showed superior performance with respect to the traditional EMPC. Finally, although we make no claim about the generality of these economic benefits where the proposed EMPC performs no worse than the traditional EMPC, the results show that microgrid operators can reduce operating electricity costs using the proposed EMPC.

¹The region of attraction is the set of initial states from which asymptotic stability of the closed-loop solution of the MPC is achieved with respect to the known reference trajectory.

The authors in [25] proved that the reference trajectory provides an upper bound on the asymptotic operating electricity costs when considering infinite time horizon EMPC problems with rolling horizon time windows. The results presented in this paper show that these results appear to carry over to finite time horizon EMPC problems as well for both shrinking and rolling horizons. Future work will focus on theoretical analysis of the asymptotic cost performance of the proposed EMPC. Further work may also consider generating a reference trajectory by solving an optimization problem with a different objective function, such as CO₂ emission reduction. Additionally, incorporating errors into the demand and PV generation forecasts is needed to evaluate the proposed algorithm in real-world implementations.

ACKNOWLEDGMENTS

We acknowledge funding from the California Energy Commission under EPC-17-049. CC acknowledges financial support from CONICYT PFCHA/DOCTORADO BECAS CHILE/2017.

REFERENCES

- [1] L. Luo, S. S. Abdulkareem, A. Rezvani, M. R. Miveh, S. Samad, N. Aljojo, and M. Pazhoohesh, "Optimal scheduling of a renewable based microgrid considering photovoltaic system and battery energy storage under uncertainty," *Journal of Energy Storage*, vol. 28, p. 101306, Apr 2020.
- [2] R. Hledik, "Rediscovering residential demand charges," *The Electricity Journal*, vol. 27, no. 7, pp. 82–96, 2014.
- [3] H. Nazarpouya, B. Wang, and D. Black, "Electric vehicles and climate change: Additional contribution and improved economic justification," *IEEE Electrification Magazine*, vol. 7, no. 2, pp. 33–39, 2019.
- [4] A. Ghosh, M. Z. Zapata, S. Silwal, A. Khurram, and J. Kleissl, "Effects of number of electric vehicles charging/discharging on total electricity costs in commercial buildings with time-of-use energy and demand charges," *Journal of Renewable and Sustainable Energy*, vol. 14, no. 3, 2022.
- [5] O. Ogunmodede, K. Anderson, D. Cutler, and A. Newman, "Optimizing design and dispatch of a renewable energy system," *Applied Energy*, vol. 287, p. 116527, 2021.
- [6] S. Mishra, J. Pohl, N. Laws, D. Cutler, T. Kwasnik, W. Becker, A. Zolan, K. Anderson, D. Ollis, and E. Elgqvist, "Computational framework for behind-the-meter der techno-economic modeling and optimization: Reopt lite," *Energy Systems*, vol. 13, no. 2, pp. 509–537, 2022.
- [7] S. Mishra and N. D. Laws, "Nrel's reopt lite tool-open source," National Renewable Energy Lab.(NREL), Golden, CO (United States), Tech. Rep., 2020.
- [8] R. Hanna, J. Kleissl, A. Nottrott, and M. Ferry, "Energy dispatch schedule optimization for demand charge reduction using a photovoltaic-battery storage system with solar forecasting," *Solar Energy*, vol. 103, pp. 269–287, 2014.
- [9] Z. Wang, B. Asghari, and R. Sharma, "Stochastic demand charge management for commercial and industrial buildings," in *2017 IEEE Power & Energy Society General Meeting*. IEEE, 2017, pp. 1–5.
- [10] M. E. Raoufat, B. Asghari, and R. Sharma, "Model predictive bess control for demand charge management and pv-utilization improvement," in *2018 IEEE Power & Energy Society Innovative Smart Grid Technologies Conference (ISGT)*. IEEE, 2018, pp. 1–5.
- [11] F. Luo, W. Kong, G. Ranzi, and Z. Y. Dong, "Optimal home energy management system with demand charge tariff and appliance operational dependencies," *IEEE Transactions on Smart Grid*, vol. 11, no. 1, pp. 4–14, 2019.
- [12] J. Leadbetter and L. Swan, "Battery storage system for residential electricity peak demand shaving," *Energy and Buildings*, vol. 55, pp. 685–692, 2012. [Online]. Available: <http://dx.doi.org/10.1016/j.enbuild.2012.09.035>
- [13] R. T. De Salis, A. Clarke, Z. Wang, J. Moyne, and D. M. Tilbury, "Energy storage control for peak shaving in a single building," *IEEE Power and Energy Society General Meeting*, vol. 2014-October, no. October, pp. 1–5, 2014.
- [14] Y.-A. Chen, R. Greenough, M. Ferry, K. Johnson, and J. Kleissl, "Value stacking of a behind-the-meter utility-scale battery for demand response markets and demand charge management: real-world operation on the uc san diego campus," in *2021 IEEE Power & Energy Society General Meeting (PESGM)*. IEEE, 2021, pp. 1–6.
- [15] R. Kumar, M. J. Wenzel, M. J. Ellis, M. N. Elbsat, K. H. Drees, and V. M. Zavala, "A Stochastic Model Predictive Control Framework for Stationary Battery Systems," *IEEE Transactions on Power Systems*, vol. 33, no. 4, pp. 4397–4406, jul 2018.
- [16] Y.-a. Chen, W. Zeng, A. Khurram, and J. Kleissl, "Cost-Optimal Aggregated Electric Vehicle Flexibility for Demand Response Market Participation by Workplace Electric Vehicle Charging Aggregators," *Energies*, vol. 17, 2024. [Online]. Available: <https://doi.org/10.3390/en17071745>
- [17] L. Yang, X. Geng, X. Guan, and L. Tong, "Ev charging scheduling under demand charge: A block model predictive control approach," *IEEE Transactions on Automation Science and Engineering*, 2023.
- [18] Z. J. Lee, G. Lee, T. Lee, C. Jin, R. Lee, Z. Low, D. Chang, C. Ortega, and S. H. Low, "Adaptive Charging Networks: A Framework for Smart Electric Vehicle Charging," *IEEE Transactions on Smart Grid*, vol. 12, no. 5, pp. 4339–4350, 2021.
- [19] A. A. Mohamed, D. Day, A. Meintz, and M. Jun, "Real-time implementation of smart wireless charging of on-demand shuttle service for demand charge mitigation," *IEEE Transactions on Vehicular Technology*, vol. 70, no. 1, pp. 59–68, 2020.
- [20] M. Ellis, H. Durand, and P. D. Christofides, "A tutorial review of economic model predictive control methods," *Journal of Process Control*, vol. 24, pp. 1156–1178, 8 2014. [Online]. Available: <https://linkinghub.elsevier.com/retrieve/pii/S0959152414000900>
- [21] A. Ghosh, C. Cortes-Aguirre, Y.-A. Chen, A. Khurram, and J. Kleissl, "Adaptive chance constrained mpc under load and pv forecast uncertainties," in *2023 IEEE PES Grid Edge Technologies Conference & Exposition (Grid Edge)*. IEEE, 2023, pp. 1–5.
- [22] G. McClone, A. Ghosh, A. Khurram, B. Washom, and J. Kleissl, "Hybrid machine learning forecasting for online mpc of work place electric vehicle charging," *IEEE Transactions on Smart Grid*, 2023.
- [23] A. Parisio, E. Rikos, and L. Glielmo, "Stochastic model predictive control for economic/environmental operation management of microgrids: An experimental case study," *Journal of Process Control*, vol. 43, pp. 24–37, 2016. [Online]. Available: <https://www.sciencedirect.com/science/article/pii/S0959152416300324>
- [24] K. Garifi, K. Baker, B. Touri, and D. Christensen, "Stochastic model predictive control for demand response in a home energy management system," in *2018 IEEE Power & Energy Society General Meeting (PESGM)*, 2018, pp. 1–5.
- [25] M. J. Risbeck and J. B. Rawlings, "Economic model predictive control for time-varying cost and peak demand charge optimization," *IEEE Transactions on Automatic Control*, vol. 65, no. 7, pp. 2957–2968, 2020.
- [26] E. Stai, C. Wang, and J.-Y. Le Boudec, "Online battery storage management via lyapunov optimization in active distribution grids," *IEEE Transactions on Control Systems Technology*, vol. 29, no. 2, pp. 672–690, 2020.
- [27] P. Grammatikos, M. Paolone, and J.-Y. Le Boudec, "Design of cost functions for the real-time control of microgrids hosting distributed energy-storage systems," *Sustainable Energy, Grids and Networks*, vol. 35, p. 101141, 2023.
- [28] D. Angeli, A. Casavola, and F. Tedesco, "Theoretical advances on Economic Model Predictive Control with time-varying costs," *IFAC-PapersOnLine*, vol. 48, no. 23, pp. 272–277, 2015. [Online]. Available: <http://dx.doi.org/10.1016/j.ifacol.2015.11.295>
- [29] SDGE, "Historical tariffs," <https://www.sdge.com/rates-and-regulations/historical-tariffs>, 2024.
- [30] N. Blair, N. Diorio, J. Freeman, P. Gilman, S. Janzou, T. W. Neises, and M. J. Wagner, "System advisor model (sam) general description (version 2017.9.5)," Tech. Rep. NREL/TP-6A20-70414, 2018.
- [31] M. Grant and S. Boyd, "Graph implementations for nonsmooth convex programs," in *Recent Advances in Learning and Control*, ser. Lecture Notes in Control and Information Sciences, V. Blondel, S. Boyd, and H. Kimura, Eds. Springer-Verlag Limited, 2008, pp. 95–110, http://stanford.edu/~boyd/graph_dcp.html.
- [32] S. Boyd and L. Vandenberghe, *Convex optimization*. Cambridge university press, 2004.
- [33] S. Boyd, S. Diamond, E. Busseti, A. Agrawal, and J. Zhang, "Convex optimization overview," https://web.stanford.edu/~boyd/papers/pdf/cvx_opt_intro.pdf.